

DFT, characterization and investigation of vibrational spectroscopy of 4-(4-hydroxy)-3-(2-pyrazine-2-carbonyl)hydrazonomethylphenyl-diazen-yl-benzenesulfonamide and its copper(II) complex



Reda A.A. Ammar^a, Abdel-Nasser M.A. Alaghaz^{b,*}, Ahmed A. Elhenawy^{b,c}

^aChemistry Department, College of Science, King Saud University, Riyadh, Saudi Arabia

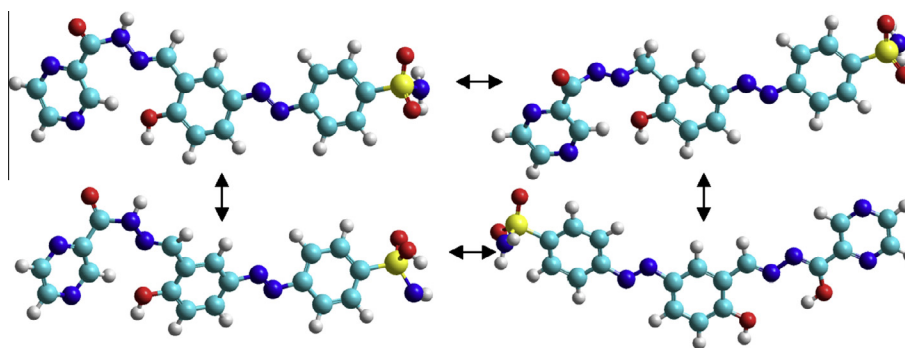
^bChemistry Department, Faculty of Science, Al-Azhar University, Nasr City, Cairo 11884, Egypt

^cChemistry Department, Faculty of Science and Arts, Al-Baha University, Al-Mukhwah, Al-Baha, Saudi Arabia

HIGHLIGHTS

- The ligand and its Cu(II) complex were synthesized and characterized.
- Spectroscopic properties of the ligand and its Cu(II) complex were carried out.
- Geometrical optimization of ligand calculated using DFT/B3LYP with 6-31G* and 6-311G** level.
- The calculated vibrational frequencies showed slight deviation from experimental frequencies for the ligand.
- The reactivity descriptors for ligand H₂L and its Cu(II) complex were computed and showed increasing dipole moment of ligand.

GRAPHICAL ABSTRACT



ARTICLE INFO

Article history:

Received 16 November 2013

Received in revised form 7 February 2014

Accepted 26 February 2014

Available online 19 March 2014

Keywords:

Azo-Schiff base

IR

EPR

Cyclic voltammetry

DFT/B3LYP

ABSTRACT

Azo-Schiff-base complex of Cu(II) has been synthesized and characterized by elemental, spectral and thermal studies. The conductance data indicate the non-electrolytic nature of the complex. The IR spectra of the prepared complex was suggested that the azo-Schiff-base ligand [4-((4-hydroxy-3-(2-(pyrazine-2-carbonyl) hydrazono)methyl)phenyl)diazen-yl)benzenesulfonamide] (H₂L) behaves as a tri-dentate ligand through the carbonyl oxygen atom, azomethine nitrogen atom and phenolic oxygen atom (ONO). The surface morphology (SEM) of the ligand and its copper(II) complex was studied using SEM analysis. X-ray powder diffraction (XRD) helps to determine the cell parameters of the complex. Transmission electron microscopy (TEM) indicated spherical particles of ~200 nm diameter. The physico-chemical studies revealed octahedral geometry around copper ion. The EPR spectra of copper complex in DMSO at 300 and 77 K were recorded and their salient feature was reported. The redox behavior of the ligand and its copper(II) complex were studied using cyclic voltammetry. Thermal properties and decomposition kinetics of copper(II) complex was investigated. The interpretation mathematical analysis and evaluation of kinetic parameters (*E*, *A*, ΔH , ΔS and ΔG) of all thermal decomposition stages have been evaluated using Coats–Redfern (CR), Horowitz–Metzger (HM) and Piloyan–Novikova (PN) equations. Moreover, the density functional theory studies are discussed for ligand, using DFT/B3LYP with 6-31G*

* Corresponding author at: Chemistry Department, Faculty of Science, Al-Azhar University, Nasr City, Cairo 11884, Egypt. Tel.: +20 1003358476.

E-mail addresses: aalajhaz@hotmail.com, aalajhaz@yahoo.com (Abdel-Nasser M.A. Alaghaz).

and 6-311G* level of theory, the absorption spectra has been computed by using time dependent at TD-DFT/B3LYP with 6-31G* and 6-311G* level of theory. The HOMO–LUMO energy gap of studied systems has been discussed.

© 2014 Elsevier B.V. All rights reserved.

Introduction

During the past two decades, considerable attention has been paid to the chemistry of the transition metal complexes of Schiff bases containing oxygen and other donors [1–6]. Schiff bases are a class of important compounds in medicinal and pharmaceutical field. They show biological activities including antibacterial [7–10], antifungal [11,12], anticancer [13–15], and herbicidal [16] activities. Furthermore, Schiff bases are utilized as starting material in the synthesis of industrial [17] and biological compounds such as β -lactons [18]. Azo compounds have been used for a long time as dyes in industry [19]. In addition, azo compounds are used in analytical chemistry as indicators in pH, redox, or complexometric titration [20,21]. Some azo compounds have shown a good antibacterial activity [22]. The existence of an azo moiety in different types of compounds has caused them to show pesticidal activity [16]. Sulfonamides are important class of drugs with several types of pharmacological agents possessing antibacterial [23], antithyroid [24], diuretic [25] and hypoglycaemic [26]. Based on the mentioned properties for Schiff base and azo compound, was reported herein the syntheses and characterization of a novel azo-dye Schiff base derivative derived from sulfanilamide and its Cu(II) complex.

Experimental

Materials

All chemicals used in the present work were of highest purity and of the analytical reagent grade (AR). The solvents used were either spectroscopic pure from BDH or purified by the recommended method [27].

The apparatus and physical measurements

The C, H, N and S data were obtained by using a Carlo-Erba 1106 elemental analyzer. Copper content was determined complexometrically by standard EDTA titration. The infrared spectra were recorded on a Shimadzu FT-IR spectrometer using KBr discs. The molar conductance measurements were carried out using a Sybron-Barnstead conductometer. The ^1H NMR (300 MHz) spectrum was recorded using 300 MHz Varian–Oxford Mercury. The deuterated solvent used was dimethylsulphoxide (DMSO) and the spectrum extended from 0 to 15 ppm. The sample was dissolved in DMSO- d_6 using tetramethylsilane as internal references. The solid reflectance spectra were measured using a Shimadzu PC3101 UV–VIS–NIR scanning spectrophotometer. Magnetic susceptibility of the copper(II) complex was measured by the Gouy method at room temperature using a Johnson Matthey, Alpha products, model MK1 magnetic susceptibility balance and the effective magnetic moments were calculated using the relation $\mu_{\text{eff}} = 2.828 (\chi_{\text{m}} T)^{1/2}$ B.M., where χ_{m} is the molar susceptibility corrected using Pascal's constants for diamagnetism of all atoms in the compounds. The ultraviolet spectra were recorded on a Perkin–Elmer Lambda–3B UV–VIS spectrophotometer. The mass spectra were performed using a Shimadzu-Ge-MS-Qp 100 EX mass spectrometer using the direct inlet system. The electron paramagnetic resonance (EPR) spectrum was recorded on a conventional X-band Bruker ELEXSYS E 500 CW-spectrometer operating at 9.5 GHz with a

100 kHz magnetic field modulation. The investigated sample was in a fine powder form [28]. Powder XRD data were collected on a PW1710 diffractometer. The operating voltage of the instrument was 30 kV and the operating current was 20 mA. The intensity data were collected at room temperature over a 2θ range of 5.025–79.925° with a continuous scan mode. Scanning electron microscope (SEM) measurements were carried out using small pieces of prepared samples on different sectors to estimate the actual molar ratios by using “TXA-840, JEOL-Japan” attached to XL30 apparatus with EDX unit, accelerant voltage 30 kV, magnification $10\times$ up to 500,000 \times and resolution 3 nm. The samples were coated with gold. Transmission electron microscopy (TEM) images were obtained on a Tecnai 30 G2S–Twin electron microscope with an accelerating voltage of 300 kV on the surface of a carbon coated copper grid. The thermal analyses (TGA and DTA) were carried out in dynamic nitrogen atmosphere (20 mL min^{-1}) with a heating rate of 10 $^{\circ}\text{C min}^{-1}$ using Shimadzu TG-50H and DTA-50H thermal analyzers.

Preparation of the Schiff base compound

Diazotization and coupling

In 1 l beaker, dissolve (56.76 g, 0.33 mol) of 4-aminobenzene-sulfonamide in 85 ml of concentrated hydrochloric acid and 85 ml of water. Cool the mixture to 0 $^{\circ}\text{C}$ in an ice–salt bath with stirring and the addition of a little crushed ice. Add during 10–15 min a solution of (24 g, 0.33 mol) of sodium nitrite in 50 ml of water, stir the solution well during the diazotization, and keep the mixture at a temperature of 0–5 $^{\circ}\text{C}$ by the addition of a little crushed ice from time to time. The very soluble diazonium salt is formed. Dissolve (40.26 g, 0.33 mol) of salicylaldehyde in a solution of 21 g of sodium hydroxide in 75 ml water, cool in ice and add the diazotized solution slowly and with stirring. Then add concentrated hydrochloric acid slowly and with constant stirring to the cold mixture until the pH of solution become 5.5. Filter the precipitated substance, 4-((3-formyl-4-hydroxyphenyl)diazonyl)benzenesulfonamide, with gentle suction, wash with water until free from acid and dried upon filter paper in the air.

Preparation of the Schiff base H_2L

The Schiff base H_2L was prepared by mixing hot solution 60 $^{\circ}\text{C}$ of 4-((3-formyl-4-hydroxyphenyl)diazonyl)benzenesulfonamide (100.75, 0.33 mol) with hot solution 60 $^{\circ}\text{C}$ of pyrazine-2-carbohydrazide (45.54 g, 0.33 mol) in 50 ml ethanol. The mixture was refluxed for 3 h. The formed solid product was separated by filtration, purified by crystallization from ethanol, washed several times with diethyl ether and dried in vacuum over anhydrous calcium chloride to give orange crystals, yield 85%.

Preparation of the copper(II) complex

Copper(II) complex of H_2L ligand was prepared by the addition of a hot solution 60 $^{\circ}\text{C}$ of the appropriate $\text{CuCl}_2 \cdot 2\text{H}_2\text{O}$ (1 mmol) in ethanol (25 ml) to the well stirred hot solution of the Schiff base (2 mmol) in the same solvent (25 ml). The mixture was left under reflux with continuous stirring for 4 h where upon the solid complex precipitated. The obtained solid was washed with ethanol followed by diethyl ether and dried in vacuum over anhydrous

Table 1
Physical data of Ligand (H_2L) and corresponding metal complexes.

Compound no. M.F. (M.Wt.)	Yield (%)	m.p. (°C)	Color	Elemental analyses % calculated (found)					μ_{eff} (B.M.)	λ ($\Omega^{-1} \text{ mol}^{-1} \text{ cm}^2$)
				M	C	H	N	S		
H_2L $C_{18}H_{15}N_7O_4S$ (425.42)	85	160–162	Orange	–	50.82 (50.78)	3.55 (3.52)	23.05 (22.99)	7.54 (7.53)	–	–
$[Cu(L)_2] C_{36}H_{28}CuN_{14}O_8S_2$ (912.37)	64	>300	Dark brown	6.96 (6.94)	47.39 (47.32)	3.09 (3.03)	21.49 (21.42)	7.03 (6.99)	2.13	1.53

calcium chloride. The analytical data of the copper(II) complex are collected in Table 1.

Computational detail

All electronic structure calculations were performed using the Spartan 08 program [28]. Geometry optimizations have been achieved using semi-empirical AM1 molecular orbital for density functional theory [29,30] with a B3LYP/6-31G* and 6-311G* basis sets [29–32]. The structural parameters, such as the dipole moment of the molecules, the energy of the highest occupied molecular orbital EHOMO and the lowest unoccupied molecular orbital ELUMO, atomic charges derive from Mulliken population analysis [33] were obtained. The vibration frequency calculation also, was computed. For each stationary point was performed at DFT with B3LYP using 6-31G* and 6-311G**, to characterize its nature as minima or transition states and to correct energies. The graphical representation of the molecular electrostatic potential surface (MEP or ESP), as implemented within the SPARTAN program [34,35].

Results and discussion

The ligand (H_2L)

The Azo-dye Schiff base ligand, H_2L has been prepared by the condensation between 4-((3-formyl-4-hydroxyphenyl)-diazenyl)benzenesulfonamide with pyrazine-2-carbohydrazide, (1:1 M ratio) in EtOH as shown in Scheme 1. The level of the purity of the ligand and the complex were checked by T.L.C. on silica gel-coated plates. H_2L Schiff base ligand give the complex with Cu(II) salt. The complex was synthesized by the general equations shown below. The ligand is stable at room temperature and soluble in common organic solvents such as DMSO, DMF, EtOH and MeOH. The complex is also stable at room temperature. Based on the

elemental analyses, spectroscopic characterization, this mononuclear complex is presumed to have the coordination environment shown in Scheme 2.

Elemental analyses

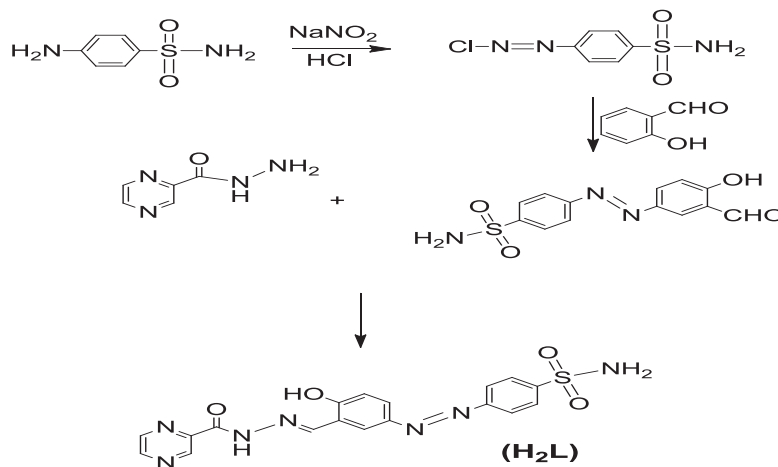
The novel Azo-dye Schiff base (H_2L) is prepared and subjected to elemental analyses, mass and IR spectral analyses. The results of elemental analyses (C, H, N, S) with molecular formula and the melting point are presented in Table 1. The results obtained are in good agreement with those calculated for the suggested formula and the melting point is sharp indicating the purity of the prepared Azo-dye Schiff base. The structure of the Azo-dye Schiff base under study is as shown in Scheme 1.

IR spectrum

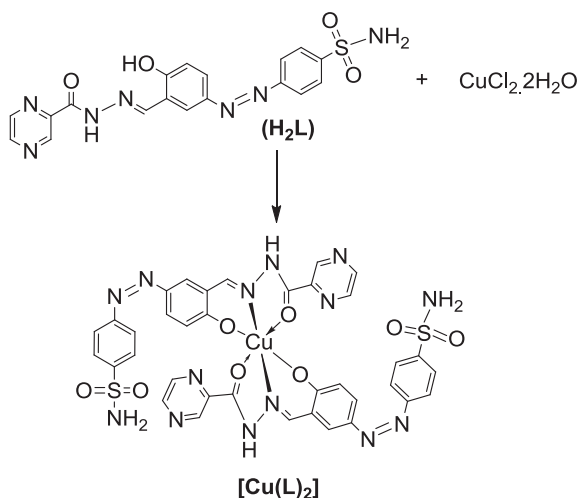
The IR spectrum (Fig. S1; Table 2) of azo-dye Schiff base ligand (H_2L) is given in synthetic procedures. Vibration bands with the wave numbers of 3522 cm^{-1} ($\nu_{\text{O-H}}$), 3075 cm^{-1} ($\nu_{\text{C-H}}$, Ar–H), 1683 cm^{-1} ($\nu_{\text{C=O}}$), 1627 cm^{-1} ($\nu_{\text{C=N}}$), 1565 cm^{-1} ($\nu_{\text{C=C}}$), 1212 cm^{-1} ($\nu_{\text{C-O}}$, Ar–O) was observed for azo-dye Schiff base ligand (H_2L). The stretching frequency observed at 2852 cm^{-1} in H_2L shows the presence of O–H–N intramolecular hydrogen bond. Schiff base ligand H_2L with strong band at 1212 cm^{-1} possesses highest percentage of enolimino tautomer due to the stabilization of phenolic C–O bond. H_2L ligand shows bands at 1435, 1325 and 1155 cm^{-1} due to $\nu_{\text{N=N}}$, $\nu_{\text{SO}_2\text{-asy}}$ and $\nu_{\text{SO}_2\text{ sym}}$, respectively.

^1H NMR spectrum

^1H NMR spectral data of the ligand (Fig. S2) relative to TMS in DMSO- d_6 without and with D_2O give further support of the suggested structure of the ligand. The broad signal at $\delta = 13.78 \text{ ppm}$ is assigned to the proton of the hydroxyl group. This peak is due to hydrogen bonded phenolic proton and the integration is generally less than 2.0 due to this intramolecular hydrogen bonding. The



Scheme 1. Synthesis of ligand (H_2L).



Scheme 2. Synthesis of Cu(II) complex of ligand (H_2L).

hydrogen proton of NH group assigned at 10.08 which disappeared with D_2O , signal for the methine proton of the characteristic azomethine group for azo-dye Schiff base, $-N=CH-$ was observed at 8.98 ppm. The shielding hydrogen atoms of amino group for SO_2NH_2 moiety at 7.83 (s, 2H, NH_2 disappeared with D_2O). In the region of 7.32–6.86 ppm chemical shifts were assigned for aromatic protons Structure S1.

Mass spectrum

The electron impact mass spectrum (Fig. S3) of the free ligand, confirms the proposed formula by showing a peak at 425 u corresponding to the ligand moiety [$(C_{18}H_{15}N_7O_4S)$ atomic mass 425 u]. The series of peaks in the range, i.e. 57, 136, 200, 250, 318 and 385u, attributable to different fragments of the ligand. These data suggest the condensation of keto group with amino group. The molecular ion peak (425 u) is in good agreement with the suggested molecular formula indicated from elemental analyses.

UV-vis spectrum

The UV-vis spectrum of the ligand (Fig. S4) show three bands in the range 223, 284 and 378 nm which can be assigned to $\pi-\pi^*$ transitions within the aromatic rings, $\pi-\pi^*$ transitions within $C=N$ and intramolecular charge transfer (CT) transition with the whole molecule.

Characterization of the metal complex

The structure of the complex was elucidated with use of IR, UV-visible spectra and elemental analyses. Conductivity value for the $[Cu(L)_2]$ compound in MeOH is at $1.53 (\Omega^{-1} \text{ cm}^3 \text{ mol}^{-1})$ indicating that they are non-electrolytes [36]. Single crystal of the compound could not be isolated from any organic solution, thus no definite structures can be described.

Elemental analyses of the complex

The results of elemental analyses, Table 1 are in good agreement with those required by the proposed formula. The data show the complexation of 1:2 [Copper:ligand] ratio of the formulae of $[Cu(L)_2]$. However, the analytical and spectroscopic data enables us to predict possible structure as shown in Scheme 2.

IR-spectra

On comparing the IR-spectra of the free ligand with the IR spectra (Fig. S1; Table 2) of their complex the following can be pointed out:

- (i) The IR spectrum of complex displayed absorption band at 1557 cm^{-1} which can be assigned to $C=N$ stretching frequency of coordinated ligand, whereas for free ligand this band was at 1577 cm^{-1} . The shift to lower frequencies (as compared to free ligand) indicated donation of the lone pair of electrons on azomethine nitrogen to copper center, this has been strengthened by the shift of $\nu(N-N)$ band at 1052 cm^{-1} in free ligand to 1025 cm^{-1} in complex.
- (ii) The νOH phenolic and νOH enolic of the free ligand is absent from the IR spectrum of the complex which indicates that, the phenolic (OH) and enolic (OH) groups contribute to the formation of complex by H^+ ions displacement [37] which points that the free ligand is considered in complex formation as monoanionic ligand.
- (iii) The bands of νNH_2 asym, νNH_2 sym, $\nu C=N$ ring, $\nu N=N$, νSO_2 asym and νSO_2 sym, in the IR spectra of the free ligand still lie at the same position in the IR spectrum of the copper(II) complex. These indicate that these groups did not contribute to the coordination of the copper ion in the complex.
- (iv) The spectrum exhibits the IR band at 1683 which may be assigned to the amide [$\nu(C=O)$] stretching vibration. On complex formation, the position of amide is shifted to the lower wave numbers [37]. This indicates that the amide oxygen atom is coordinated to the copper ion.
- (v) For the copper(II) complex two new bands appear in their IR spectrum at 336 cm^{-1} and 292 cm^{-1} respectively, which are absent from the IR spectrum of the free ligand, these can be assigned to $\nu Cu-O$ and $\nu Cu-N$ bands, respectively [37].

Mass spectrum of copper(II) complex

The mass spectrum of complex (Fig. S3) showed peaks attributed to the molecular ions m/z at $912 M^+$ for copper(II) complex. This data is in good agreement with the proposed molecular formula for this complex i.e. $[Cu(L)_2]$. The purity of the ligand and their complex was checked using LC-mass technique. This confirms the formation of the Schiff-base frame.

Electronic, magnetic and ESR spectral studies

The electronic spectral data of the free ligand and Cu(II) complex, in the range 200–400 and 200–700 nm, respectively, in DMF solvent as well as their magnetic susceptibility (μ_{eff}) and molar conductance values are displayed in Table 1. Electronic spectrum of the free ligand in DMF solution displayed two absorption bands at $35,211$ and $26,455 \text{ cm}^{-1}$, the first band could be attributed to the $\pi \rightarrow \pi^*$ transition of the azomethine group (K-band), and the second band might arise from the $n \rightarrow \pi^*$ transitions resulting from nitrogen and oxygen atoms (R-band) [34]. These bands exhibit more or less shift in complexes.

The observed magnetic moment of the Cu(II) complex is 2.13 B.M., which confirms the octahedral structure of this complex [38,39]. The electronic spectrum of the Cu(II) complex (Fig. S4) gave a band at $11,788 \text{ cm}^{-1}$ ($\epsilon = 56 \text{ L mol}^{-1} \text{ cm}^{-1}$), $18,312 \text{ cm}^{-1}$ ($\epsilon = 94 \text{ L mol}^{-1} \text{ cm}^{-1}$) and $21,300 \text{ cm}^{-1}$ ($\epsilon = 152 \text{ L mol}^{-1} \text{ cm}^{-1}$), these bands may be assigned to ${}^2B_{1g} \rightarrow {}^2B_{2g}$, ${}^2B_{1g} \rightarrow {}^2A_{1g}$ and ${}^2B_{1g} \rightarrow {}^2E_g$ transitions, respectively, another band observed at $21,300 \text{ cm}^{-1}$ suggesting the existence of a transition from dxy , dz^2 and dxz , dyz transfer to the antibonding and half-filled $dx^2 - dy^2$ level which is consistent with an octahedral configuration.

The X-Band ESR spectrum of $[Cu(L)_2]$ complex at room temperature was shown in (Fig. S5). The spectrum of the Cu(II) complex exhibits two broad bands with $g_{\parallel} = 2.16$ and $g_{\perp} = 2.05$ so,

Table 2
Experimental and computational calculated vibrational wavenumbers (harmonic frequency (cm^{-1})), IR intensities and assignments for HMQ at B3LYP utilizing 6-31G* and 6-311G** basis sets of H_2L ligand and its Cu(II) complex with their assignments.

Assignments	(H ₂ L) Exp.	B3LYP/6-31G*		B3LYP/6-311G**		Cu(II) Exp. IR Intensity
		Wave number	IR Intensity	Wave number	IR Intensity	
v(OH) _{phenolic}	3545br	3614	140	3579	185.02	–
v(OH) _{enolic}	2975br	3330	9.17	3432	133.90	–
vas(NH ₂)	3312br	3471	122	3518	147.01	3312br
vs(NH ₂)	3282br	3385	136	3345	74.45	3280br
vas(NH)	3271br	3388	122	3188	74.54	3271br
vs(NH)	3199br	3386	94	3145	54.65	3199br
p(NH)	1567m	1669	21.33	1554	29.54	1567m
v(C=N) _{azomethine}	1577m	1581	19.60	1535	28.45	1557m
v(C=O)	1683m	1687	4.85	1650	81.5	1669m
v(C–O)	1212m	1217	64.15	1216	21.44	1202m
v _{as} (SO ₂)	1325s	1241	54.08	1322	5.62	1322s
v _s (SO ₂)	1155m	1149	11.11	1156	221.36	1155m
v(N=N)	1435s	1459	270.26	1449	123.32	1434s
v(N–N)	1052s	1029	128.36	1089	33.91	1025m
v(C–H) _{aromatic}	3075m	3356	7.44	3113	59.36	3074m
v(C=C) _{phenyl}	1565m	1581	19.60	1594	69.9	1565m
δ(O–M–O)	–	–	–	–	–	189 w
δ(O–M–N)	–	–	–	–	–	218w
v(M–N)	–	–	–	–	–	292m
v(M–O)	–	–	–	–	–	336m

Where br = broad, s = strong, m = medium, w = weak.

$g_{\parallel} > g_{\perp} > 2.0023$, indicating that the unpaired electron of Cu(II) ion is localized in the $dx^2 - y^2$ orbital [40]. In axial symmetry, the g -values are related to the G -factor by the expression $G = (g_{\parallel} - 2) / (g_{\perp} - 2) = 4$. According to Hathaway and Billing [41]. The G values of the Cu(II) complex are < 4 suggesting that the considerable exchange interaction in the solid state. Further, the shape of the ESR spectrum of Cu(II) complex indicates that the geometry around the Cu(II) ions are elongated octahedron [42,43]. Molecular orbital coefficients, α^2 and β^2 were calculated as described previously [44]. The lower value of α^2 (0.43) compared to β^2 (1.02) in Cu(II) complex indicate that the covalent in-plane σ -bonding is more pronounced than the covalent in-plane π -bonding character.

Electrochemical behavior

Cyclic voltammetry is the most widely used technique for acquiring qualitative information about electrochemical reactions. It offers a rapid location of redox potentials of the electro active species. The cyclic voltammograms of ligand and its copper complex (Fig. S6) were recorded at 300 K in DMF solution in the potential range -1.0 to 1.3 V with scan rate 0.1 V/s.

The Azo-dye Schiff base ligand shows one irreversible couple with $E_{pc} = -0.93$ V vs Ag/AgCl and the associated anode peak at $E_{pa} = 0.17$ V. The large separation $\Delta E = 0.76$ V indicates irreversible couple. The Cu(II) complex shows irreversible cathodic peak at $E_{pc} = 0.62$ V vs Ag/AgCl corresponding to Cu(II)/(III) couple and the associated anode peak at $E_{pa} = -0.54$ V corresponding to the formation of Cu(II)/I couple. The peak to peak separation ΔE is 1.16 V confirming the process as irreversible.

Powder X-ray diffraction spectroscopy

Single crystals of the ligand and its copper complex could not be prepared to get the XRD and hence the powder diffraction data (Fig. S7) were obtained for structural characterization. Structure determination by X-ray powder diffraction data has gone through a recent surge since it has become important to get to the structural information of materials, which do not yield good quality single crystals. The indexing procedures were performed using (CCP4, UK) CRYSFIRE program [45] giving cubic crystal system for $[\text{Cu}(\text{L})_2]$ having $M(9) = 13$ as the best solution. Their cell parameters are shown in Table 3.

Table 3
Crystallographic data for the azo-dye Schiff base complex $[\text{Cu}(\text{L})_2]$.

Data	$[\text{Cu}(\text{L})_2]$
Empirical formula	$\text{C}_{36}\text{H}_{28}\text{CuN}_{14}\text{O}_8\text{S}_2$
Formula weight (g/mol)	912.37
Wavelength (Å)	1.54044
Crystal system	Cubic
Space group	$P4/m$
Unit cell dimensions (Å, °)	
a (Å)	16.1045
b (Å)	16.1045
c (°)	16.1045
α (°)	90
β (°)	90
γ (°)	90
Volume (Å ³)	5168.15
(Calc.) density (g/cm ⁻³)	1.24
2θ range	16.12–63.65
Limiting indices	$3 \leq h \leq 10, 1 \leq k \leq 6, 3 \leq l \leq 10$
Z	6
R _f	0.000011
Temperature (K)	298

Scanning electron microscopy

The SEM pictures of H_2L and $[\text{Cu}(\text{L})_2]$ are shown in Figs. S8a and b, respectively. SEM image of azo-dye Schiff base ligand, H_2L (Fig. S8a) displays more extensive three-dimensional network than the smooth lacunose surface of the benzenesulfonamide and this might be due to chemical modification of benzenesulfonamide through the condensation of pyrazine-2-carbohydrazide with free amino groups available on azo-dye Schiff base ligand surface. Because of this modification, particle sizes of the ligand, H_2L get successively reduced, which further increases the adsorption capacity towards the copper ion by complex formation. The surface of $[\text{Cu}(\text{L})_2]$ (Fig. S8b) do not exhibits the same morphology compared to that of H_2L . The difference in the morphology of H_2L and the complex could be due to the imprinting of the copper ion on the modified azo-dye Schiff base ligand (H_2L) which leaves the footprints on the surface of the complex and thus increase in the porosities is occurred on the surface of the complex. This characteristic may be assigned to the coordination of the copper ion with the active sites of H_2L .

Table 4
Kinetic parameters of [Cu(L)₂]:

Stage	Using Coats–Redfern equation					
	Decomposition range (°C)	A(S ⁻¹)	E _a (kJ/mol)	ΔH (kJ/mol)	ΔS (kJ/mol K)	ΔG (kJ/mol)
1st	465	3.07 × 10 ⁹	43.65	55.15	-0.030	167
2nd	577	5.44 × 10 ¹¹	72.07	76.86	-0.072	186
3rd	800	2.22 × 10 ⁶	111.76	106.98	-0.096	199
Using Horowitz–Metzger equation						
1st	465	2.89 × 10 ⁹	42.13	54.23	-0.030	165
2nd	577	4.99 × 10 ¹¹	70.26	72.87	-0.071	183
3rd	800	2.87 × 10 ⁶	110.24	105.45	-0.093	194
Using Piloyan–Novikova equation						
1st	465	3.04 × 10 ⁹	40.44	52.46	-0.031	163
2nd	577	5.42 × 10 ¹¹	71.79	73.78	-0.070	184
3rd	800	2.87 × 10 ⁶	110.57	102.67	-0.093	195

Transmission electron microscopy

TEM image for the Cu(II) complex is given in Fig. S9. The morphology of complex was observed to have spherical particles of 43 nm average diameter. This is lying in good agreement with the calculated value (37 nm) obtained from Scherrer's equation.

Kinetics of thermal decomposition

Recently, there has been increasing interest in determining the rate-dependent parameters of solid-state non-isothermal decomposition reactions by analysis of TG curves [23,24]. Thermogravimetric (TG) and differential thermogravimetric (DTG) analyses was carried out for Cu(II) complex in ambient conditions. The correlations between the different decomposition steps of the complex with the corresponding weight losses are discussed in terms of the proposed formula of the complex.

The complex [Cu (L)₂] with the molecular formula [C₃₆H₂₈N₁₄O₈S₂Cu] is thermally decomposed in two successive decomposition steps (Fig. S10). The first estimated mass loss of 44.72% (calculated mass loss = 44.63%) within the temperature range 540–590 K may be attributed to the loss of (C₁₈H₁₄N₇O₃S) fragment. The DTG curve gives an exothermic peak at 553 K (the maximum peak temperature). The second step occurs within the temperature range 661–853 K with the estimated mass loss 46.51% (calculated mass loss = 46.44%) which corresponds to the loss of C₁₈H₁₄N₇O₄S fragment leaving CuO as residue. The DTG curve gives an exothermic

peak at 770 K (the maximum peak temperature). Total estimated mass loss is 91.23% (calculated mass loss = 91.18%).

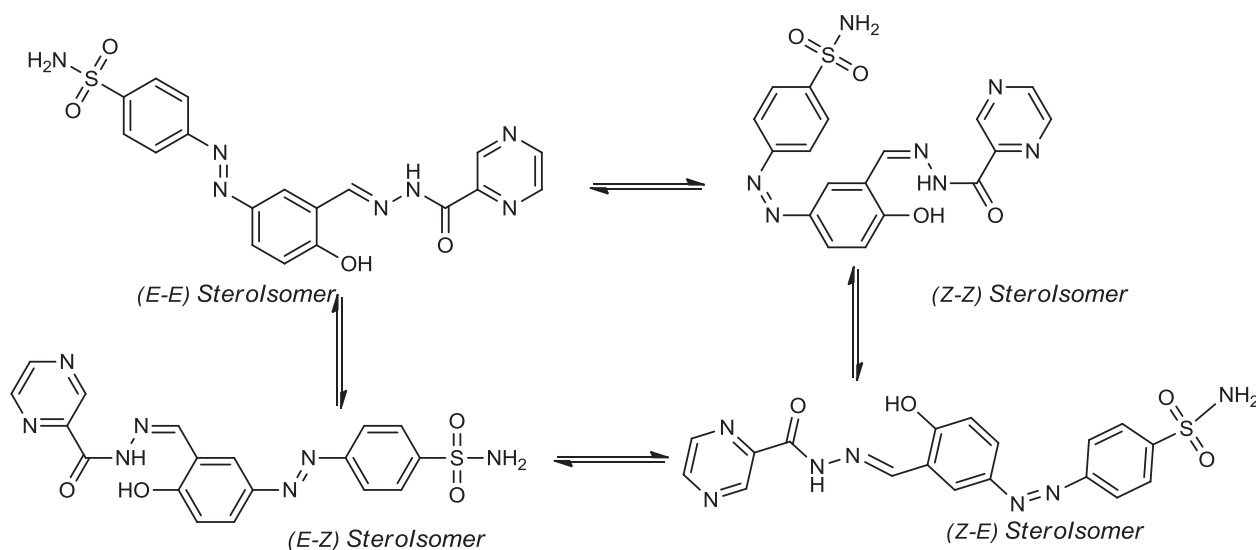
The thermodynamic activation parameters of decomposition processes of dehydrated complexes namely activation energy (*E*), enthalpy (*ΔH*), entropy (*ΔS*) and free energy of decomposition (*ΔG*) (Table 4), were evaluated by employing the Horowitz–Metzger [46] (HM), Coats–Redfern [47] (CR), and Piloyan–Novikova [48] (PN) methods and were helpful in assigning the strength of the complexes. According to the kinetic data obtained from the TG curves, all the complexes have negative entropy which indicates that the complex is formed spontaneously. The negative value of entropy also indicates a more ordered activated state that may be possible through the chemisorption of oxygen and other decomposition products. The negative values of the entropies of activation are compensated by the values of the enthalpies of activation, leading to almost the same values for the free energy of activation [49].

Computational studies

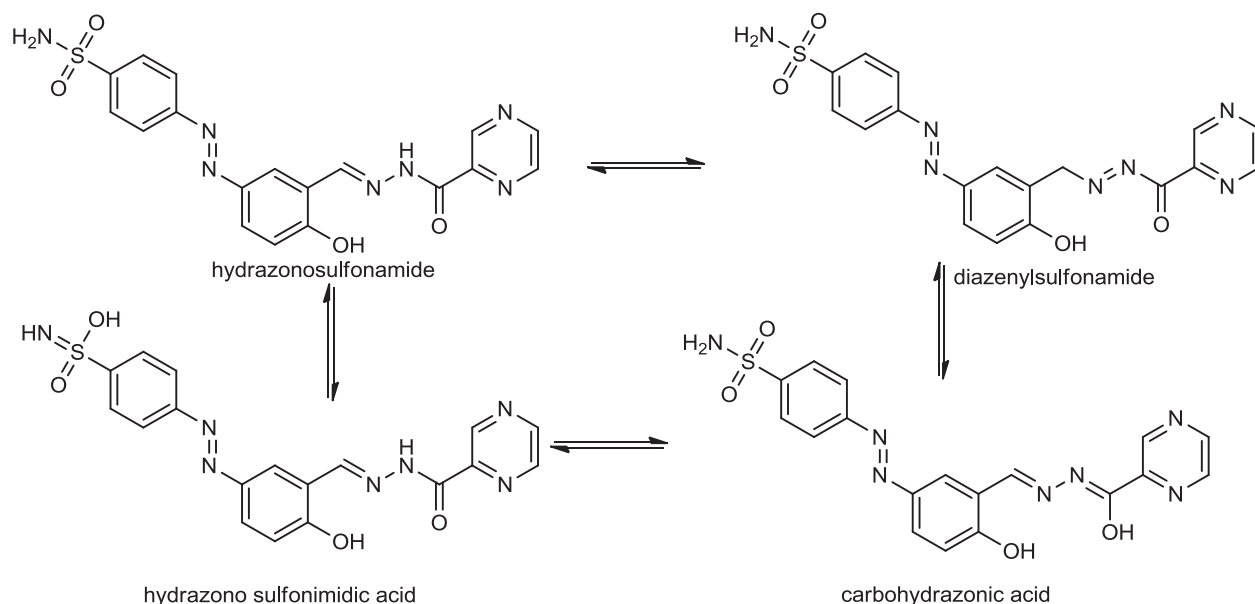
It is clearly that, a possibility existence of the prepared ligand in the stereoisomer forms were depicted in Scheme 3.

The major tautomeric structures for the ligand were represented in Scheme 4.

In order to achieve the better insight into the molecular structure of the most preferentially stereoisomer and/or tautomeric



Scheme 3. Stereoisomers of ligand.



Scheme 4. Proposed tautomer structures of most stable stereoisomer ligand.

Table 5

Calculated energies of possible stereo isomers and tautomer forms of ligand at B3LYP utilizing 6-31G* and 6-311G** basis sets.

Cpd.	E	HF	HOMO	LUMO	Dipole	ZPE
6-31G*						
(E-E)	-9184.13	49.30732	-9.30446	-0.92831	2.31762	202.06
(Z-Z)	-8789.65	53.07945	-9.22826	-1.4131	5.799222	202.46
(E-Z)	-8489.07	73.76387	-8.9824	-1.12168	9.216577	202.03
(Z-E)	-8445.16	53.89782	-9.184	-1.42712	8.842497	202.06
(E-E)a	-9140.90	53.72245	-9.60642	-1.33573	7.766137	202.04
(E-E)b	-8829.23	53.90171	-9.41322	-1.3042	6.014287	202.09
(E-E)c	-8452.00	44.97201	-9.55931	-1.73782	8.842496	202.03
6-311G**						
(E-E)	-9081.96	151.6332	-9.02917	-1.31209	7.187144	222.12
(Z-Z)	-8816.27	153.6283	-9.42276	-1.65030	3.313277	222.10
(E-Z)	-8493.96	154.1982	-9.18962	-1.38296	9.532563	222.12
(Z-E)	-8429.24	136.0901	-9.25689	-1.64373	6.25245	222.12
(E-E)a	-9053.27	158.858	-9.60390	-1.71561	8.801717	222.14
(E-E)b	-8691.51	149.3277	-9.43391	-1.67879	8.402874	222.11
(E-E)c	-8409.68	149.3631	-9.34235	-1.45775	9.615270	222.16

E: The total energy (kcal/mol), HF: heat of formation (kcal/mol), HOMO: highest occupied molecular orbital (eV), LUMO: lowest occupied molecular orbital (eV), Dipole: dipole moment calculate, ZPE: Zero point energy (kcal/mol).

forms for ligand **H₂L**, conformational analysis of the target compounds have been performed using Spartan 08 program [28] with AM1 semi-empirical molecular orbital for density functional theory [29] with a B3LYP/6-31G* and 6-311G** basis sets [29–32]. The computed molecular parameters, total energy, electronic energy, heat of formation, the highest occupied molecular orbital (HOMO) energies, the lowest unoccupied molecular orbital (LUMO) energies and the dipole moment for studied compounds were calculated, which have been used to investigate the most stable stereoisomer form and/or tautomer structure of the prepared ligand (Table 5). The minimal optimization energy of most stable stereoisomer forms and major tautomer structures for ligand were represented at (Fig. S11).

The calculated molecular parameters showed, the most stable stereoisomer is the (E-E) form and most stable tautomer structure is hydrazone-sulfonamide H₂L, this may be explained by presence the intra-molecular interaction of H-hydroxyl moiety with N-imino moiety, and owing to slightly reduces it's calculated energy, and leads to predominance this structures (E-E and hydrazone-sulfonamide H₂L) over other forms. The E-E

isomer is stabilizing by adjusting two phenyl rings in plane with each other, as the same time with pyrazine ring. The bond length for PhNNPh (H₂L) is equal for four tautomeric structures 1.266 Å (Fig. S12). The decreasing bond length of PhCHN (~1.27) for hydrazonesulfonamide than PhCHN (~1.47) of diazenylsulfonamide may be due to extension conjugated π electron of the phenyl ring (Table S1 in Supplementary material). Another evidence supported explanation, the N_{hydrazoneyl} atom with sp² hybrid orbitals has more s-character, and the maximum of the electron density is closer to the nuclei compared with the electron density distribution at sp³ hybridized N_{diazenyl} atom, which leads to lengthening the PhCN_{diazenyl} bonds (Table S1 in Supplementary material).

Comparison of the vibrational frequencies calculated at DFT/B3LYP level utilizing 6-311G basis set with experimental values (Fig. S13, Table 2). There assumable deviations between the experimental values and calculated, may be due to the fact that, the calculations have been actually performed on a single molecule in the gaseous state contrary to the experimental values recorded in the presence of intermolecular interactions.

Table 6The optimized calculations energies and reactivity descriptor parameters for ligand H₂L at B3LYP/6-311G** basis sets and Cu(II) complex at AM1 semi-empirical.

CPD	E	H.F.	HOMO	LUMO	ΔG	H	S	χ	μ	ω	D
H ₂ L	−9081.96	24.46	−9.01	−1.42	7.58	3.79	0.26	−5.22	5.22	3.59	8.14
[Cu(L) ₂]	−250186	63.14	−8.48	−1.43	7.06	3.53	0.28	−4.95	4.95	3.47	7.06

E: The total energy (kcal/mol), H.F.: heat of formation (kcal/mol), HOMO: highest occupied molecular orbital (eV), LUMO: lowest occupied molecular orbital (eV), HLG: difference between HOMO and LUMO energy levels (eV), η: Hardness (eV), S: Softness (eV), χ: electronegativity (eV), μ: chemical potential (eV), ω: electrophilicity (eV), D: dipole moment (Debye).

Table 7Mulliken q(M) charges for H₂L at using DFT/B3LYP with 6-311G** basis set and AM1 semi-empirical for complex [Cu(L)₂].

Atom	q(M)	Atom	q(M)	Atom	q(M)	Atom	q(M)
H ₂ L							
1 C0:	−0.614	41 H11:	+0.284	35 C34	−0.252	75 H14	+0.062
2 C1:	+0.015	42 H12:	+0.081	36 C35	+0.127	76 H15	+0.080
3 C2:	−0.128	43 H13:	+0.031	37 S36	+2.839	77 H16	+0.158
4 C3:	+0.476	44 H14:	+0.073	38 O37	−1.036	78 H17	+0.169
5 C4:	−0.382	45 H15:	+0.392	39 O38	−1.037	79 H18	+0.081
6 C5:	−0.015	[Cu(L) ₂]		40 N39	−1.101	80 H19	+0.344
7 S6:	+2.550			41 N40	−0.265	81 H20	+0.342
8 O7:	−0.971	1 C0	−0.503	42 N41	−0.135	82 H21	+0.092
9 O8:	−0.976	2 C1	+0.022	43 C42	+0.263	83 H22	+0.136
10 N9:	−0.946	3 C2	−0.266	44 C43	−0.033	84 H23	+0.145
11 N10:	−0.273	4 C3	+0.396	45 C44	−0.505	85 H24	+0.113
12 N11:	−0.236	5 C4	−0.282	46 C45	+0.566	86 H25	+0.327
13 C12:	+0.514	6 C5	+0.014	47 C46	−0.183	87 H26	+0.096
14 C13:	−0.535	7 S6	+2.576	48 C47	−0.284	88 H27	+0.031
15 C14:	+0.001	8 O7	−0.977	49 C48	+0.174	89 H28	+0.053
16 C15:	+0.247	9 O8	−0.976	50 N49	+0.294		
17 C16:	−0.213	10 N9	−0.967	51 N50	−0.673		
18 C17:	−0.288	11 N10	−0.293	52 C51	+0.547		
19 C18:	+0.373	12 N11	−0.141	53 O52	−0.488		
20 N19:	−0.469	13 C12	+0.294	54 C53	+0.263		
21 N20:	−0.186	14 C13	−0.285	55 C54	+0.175		
22 C21:	+0.477	15 C14	−0.354	56 N55	−0.458		
23 O22:	−0.516	16 C15	+0.567	57 N56	−0.499		
24 C23:	+0.338	17 C16	−0.365	58 C57	+0.309		
25 C24:	+0.120	18 C17	−0.052	59 C58	+0.136		
26 N25:	−0.430	19 C18	+0.205	60 O59	−0.439		
27 N26:	−0.492	20 N19	+0.198	61 Cu1	+0.202		
28 C27:	+0.284	21 N20	−0.632	62 H1	+0.108		
29 C28:	+0.084	22 C21	+0.486	63 H2	+0.151		
30 O29:	−0.519	23 O22	−0.466	64 H3	+0.166		
31 H1:	+0.122	24 C23	+0.310	65 H4	+0.107		
32 H2:	+0.199	25 C24	+0.153	66 H5	+0.303		
33 H3:	+0.201	26 N25	−0.466	67 H6	+0.298		
34 H4:	+0.119	27 N26	−0.499	68 H7	+0.131		
35 H5:	+0.297	28 C27	+0.321	69 H8	+0.170		
36 H6:	+0.298	29 C28	+0.118	70 H9	+0.100		
37 H7:	+0.258	30 O29	−0.407	71 H10	+0.118		
38 H8:	+0.137	31 C30	−0.757	72 H11	+0.323		
39 H9:	+0.214	32 C31	+0.128	73 H12	+0.100		
40 H10:	+0.031	33 C32	−0.238	74 H13	+0.026		

The computed vibrations to O–H aromatic (3614 and 3330 cm^{−1}) at B3LYP/31G*, and (3579 and 3432 cm^{−1}) with B3LYP/6-311G** basis set, respectively, have shown a comparable agreement with our experimental results.

The calculated vibrations for (νNH₂asym) of H₂L assigned at B3LYP utilizing 6.31G* set are 3471, 3385, 3388 and 3386 cm^{−1}, and using 6.311G** set exhibit vibrational bands at 3518, 3345, 3188 and 3145 cm^{−1}, which agreement our experimental results 3312 cm^{−1} (νNH₂asym), 3282 cm^{−1} (νNH₂sym), 3075 cm^{−1}.

The present work displayed computed vibrations to C=O stretching vibrations at 1687 cm^{−1} and at 1650 cm^{−1} at B3LYP utilizing 6-31G* and 6-311G** basis sets respectively which have shown a comparable agreement with our experimental results at 1683 cm^{−1}.

The computed vibrations for ν(C=N)_{azomethine} at 1581 cm^{−1} and at 1535 cm^{−1} at B3LYP utilizing 6-31G* and 6-311G** basis sets

respectively which have shown a comparable agreement with experimental results at 1577 cm^{−1}.

The lowest minimization energy for Cu(II) complex exhibited a common feature:

- I. The higher HOMO energy values show the molecule is a good electron donor, in other hand, the lower HOMO energy values indicate that, a weaker ability of the molecules for donating electron. LUMO energy presents the ability of a molecule for receiving electron (Tables 5 and 6).
- II. Phenyl and pyrazine rings, showing highly free rotations, two phenyl rings for ligands formed complex were stabilized by arranged in plane with each other and co-planner with pyrazine ring, its phenyl rings approximately arranged coplanar with the metal core of complex (Figs. S1 and S2 in Supplementary material).

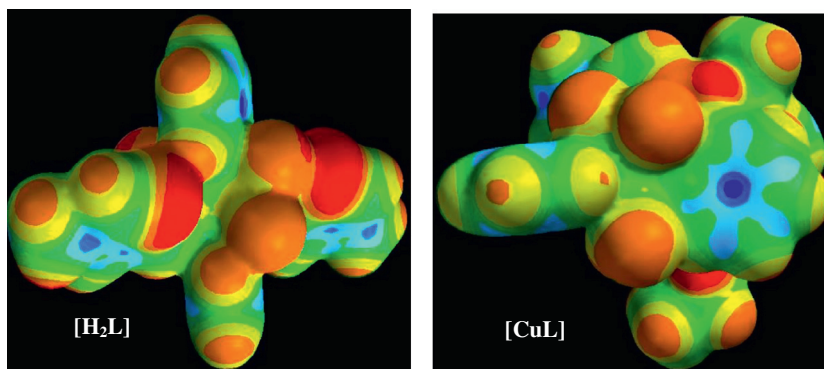


Fig. 1. The ESP surfaces for H_2L with based on DFT-B3LYP /6-311G** and AM1 semi-empirical for complex $[Cu(L)_2]$ calculations.

- III. The bond lengths of all the active groups taking part in coordination are longer than that already exist in the ligand.
- IV. The bond angles of the $N_{17}-N_{18}-C_{19}$ fragment, changed due to coordination; which are altered from 120° on ligand to 121.12° for complex.
- V. All bond angles in complex are quite near to an octahedral geometry predicting sp^3d^2 hybridization.
- VI. Furthermore, the global and local chemical reactivity descriptors for molecules have been defined (Table 6), like softness (measures stability of molecules and chemical reactivity, hardness (reciprocal of softness), chemical potential, electronegativity (strength atom for attracting electrons to itself), electrophilicity index (measuring lowering energy due to maximal flowing electron between donor and acceptor) [50–55]. The results were concluded, the complex have lower energy gap, higher softness (most stable), lower hardness, higher chemical potential and higher electrophilicity. The lower dipole moment value for Cu(II) 7.06 Debye than ligand 8.14 Debye, indicate ability interaction of ligand with the metal to form complex.
- VII. The Mulliken $q(M)$, charges were computed within full Bond Orbital analysis at with B3LYP/6-311G** for the most stable ligand H_2L and AM1 semiempirical for $[Cu(L)_2]$ are shown in (Table 7). The charge distributions over the atoms suggest that, the formation of donor and acceptor pairs involving the charge transfer in the molecule. In general in both compounds, the hydrogen, Copper and some carbon atoms are positively charged, the O and N atoms have negative charges, and accepted the electrons. The complexation with copper metal ion leads to a redistribution of electron density of molecule (S Table 3 in Supplementary material). The most negative centers in H_2L and $[Cu(L)_2]$ involved in oxygen of sulfonyl group, on the other hand the most positive charge are located on the S of sulfonyl group, the maximum positive charge on the C1 atom are due to attachment of the electronegative oxygen atom (withdrawing nature).
- VIII. The electrostatic potentials mapped (ESP) (Fig. 1) was drawn, it represents a balance between repulsive interactions of the nuclei (positively-charged) and attractive interactions for the electrons (negatively-charged). The colors toward red depict negative potential (high electron density area, representing a strong attraction between the proton and the points on the molecular surface), while colors toward blue depict positive potential, and colors in between (orange, yellow, green) depict intermediate values of the potential. Comparison of the electrostatic mappings of H_2L and its complex $[Cu(L)_2]$ showed, increasing negative charges (in red) located on the surface of complex $[Cu(L)_2]$

and increasing the polar area, decreasing polar area (in green) on surface for Ligand H_2L , these results indicate the importance of polarity surface for activity of complexes.

Conclusion

Our proposed structure of azo-dye Schiff base ligand on the basis of the IR, 1H NMR, EI mass, UV–vis. spectra has potential binding sites towards the copper ion and act as tridentate chelate by coordinating through carbonyl oxygen, hydroxyl oxygen and azomethine nitrogen. Spectral characterizations of the new complex showed that Cu(II) form six coordinate distorted octahedral complex with 1:2 (copper:ligand) stoichiometry. The most stable form of ligand are optimized using DFT/B3LYP with 6-31G* and 6-311G** level. The calculated frequencies showed slight deviation from experimental frequencies for the ligand and supported the structure. The high dipole moment value for ligand 8.14 is showed increasing its ability to interact with the surrounding environment.

Acknowledgment

This project was supported by King Saud University, Deanship of Scientific Research, College of Science Research Center.

Appendix A. Supplementary material

Supplementary data associated with this article can be found, in the online version, at <http://dx.doi.org/10.1016/j.molstruc.2014.02.051>.

References

- [1] X. Tai, X. Yin, Q. Chen, M. Tan, *Molecules* 8 (2003) 439–443.
- [2] M. Sonmez, A. Levent, M. Sekerci, *Russ. J. Coord. Chem.* 30 (9) (2004) 655–660.
- [3] M. Tuncel, S. Serin, *Synth. React. Inorg. Met. Org. Nano Met. Chem.* 35 (2005) 203–212.
- [4] A.A. Khandar, K. Nejati, Z. Rezvani, *Molecules* 10 (2005) 302–309.
- [5] A.D. Garnovskii, I.S. VasilChenko, *Russ. Chem. Rev.* 71 (2002) 943–954.
- [6] A.D. Garnovskii, A.L. Nivorozhkin, V.I. Minkin, *Coord. Chem. Rev.* 126 (1993) 1–69.
- [7] F.D. Karia, P.H. Parsania, *J. Chem. Soc.* 11 (3) (1999) 991–995.
- [8] P.G. More, R.B. Bhalvankar, S.C. Pattar, *J. Indian Chem. Soc.* 78 (9) (2001) 474–475.
- [9] A.H. El-masry, H.H. Fahmy, S.H.A. Abdelwahed, *Molecules* 5 (2000) 1429–1438.
- [10] M.A. Baseer, V.D. Jadhav, R.M. Phule, Y.V. Archana, Y.B. Vibhute, *Orient. J. Chem.* 16 (3) (2000) 533–542.
- [11] S.N. Pandeya, D. Sriram, G. Nath, E. De Clercq, *IL Farmaco* 54 (1999) 624–628.
- [12] W.M. Singh, B.C. Dash, *Pesticides* 22 (11) (1988) 33–37.
- [13] E.M. Hodnett, W.J. Dunn, *J. Med. Chem.* 13 (1970) 768–770.
- [14] S.B. Desai, P.B. Desai, K.R. Desai, *Heterocycl. Commun.* 7 (1) (2001) 83–90.
- [15] P. Pathak, V.S. Jolly, K.P. Sharma, *Orient. J. Chem.* 16 (1) (2000) 161–162.
- [16] S. Samadhiya, A. Halve, *Orient. J. Chem.* 17 (1) (2001) 119–122.
- [17] F. Aydogan, N. Ocal, Z. Turgut, C. Yolacan, *Bull. Korean Chem. Soc.* 22 (2001) 476–480.

- [18] A.E. Taggi, A.M. Hafez, H. Wack, B. Young, D. Ferraris, T. Lectka, *J. Am. Chem. Soc.* 124 (2002) 6626–6635.
- [19] K. Hansongnorn, S. Tempiam, J.C. Liou, F.L. Laio, T.H. Lu, *Anal. Sci.* 19 (2003) 13–16.
- [20] P.L. Coort, M. Johansson, *Electroanalysis* 12 (2000) 565–571.
- [21] D. Choi, S.K. Lee, T.D. Chung, H. Kim, *Electroanalysis* 12 (2000) 477–482.
- [22] P. Alka, P. Vinod, V.S. Jolly, *Orient. J. Chem.* 10 (1) (1994) 73–74; *J. Drews, Science* 287 (5460) (2000) 1960–1964.
- [23] C.W. Thornber, *Chem. Soc. Rev.* 8 (1979) 563–580.
- [24] C.T. Supuran, A. Scozzafava, *Exp. Opin. Ther. Patents* 10 (26) (2000) 575–600.
- [25] T.H. Maren, *Annu. Rev. Pharmacol. Toxicol.* 16 (1976) 309–327.
- [26] A.E. Boyd, *Diabetes* 37 (1988) 847–850.
- [27] A.M. Tawfik, M.A. El-ghamry, S.M. Abu-El-Wafa, N.M. Ahmed, *Spectrochim. Acta A* 97 (2012) 1172–1180.
- [28] Spartan 08, Wave function Inc., Irvine, CA 92612, USA, 2008.
- [29] P. Hohenberg, W. Kohn, *Phys. Rev.* B136 (1964) 864–873.
- [30] W. Kohn, L.J. Sham, *Phys. Rev.* A140 (1965) 1133–1138.
- [31] W.J. Hehre, L. Radom, P.V.R. Schleyer, J.A. Pople, *Ab Initio Molecular Orbital Theory*, John Wiley & Sons, New York, 1986.
- [32] J. Sauer, *Chem. Rev.* 89 (1989) 199–255.
- [33] J.J.P. Stewart, *J. Comput. Chem.* 10 (1989) 209–220.
- [34] U.C. Singh, P.A. Kollman, *J. Comput. Chem.* 5 (1984) 129–145.
- [35] M.L. Connolly, *Science* 221 (1983) 709–713.
- [36] W.J. Geary, *Coord. Chem. Rev.* 7 (1971) 81–122.
- [37] K. Nakamoto, *Infrared and Raman Spectra of Inorganic and Coordination Compounds*, fourth ed., Wiley Interscience, New York, 1986.
- [38] B. Garcia, A.M. Lozano-Vila, F. Luna-Giles, R. Pedrero-Marin, *Polyhedron* 25 (2002) 1399–1407.
- [39] G. Speier, J. Csihony, A.M. Whalen, C.G. Pierpont, *Inorg. Chem.* 35 (1996) 3519–3524.
- [40] M. Sebastian, V. Arun, P.P. Robinson, A.A. Varghese, R. Abraham, E. Suresh, K.K.M. Yusuff, *Polyhedron* 29 (2010) 3014–3020.
- [41] B.J. Hathaway, D.E. Billing, *Coord. Chem. Rev.* 5 (1970) 143–207.
- [42] A. Bencini, D. Gatteschi, *EPR of Exchange Coupled Systems*, Springer-Verlag, Berlin, 1990.
- [43] O.M.I. Adly, A. Taha, S.A. Fahmy, *J. Mol. Struct.* 1054–1055 (2013) 239–250.
- [44] A.M.A. Alaghaz, R.A. Ammar, *Eur. J. Med. Chem.* 45 (2010) 1314–1322.
- [45] R. Shirley, *The CRYSFIRE System for Automatic Powder Indexing: Users Manual*, Lattice Press, 2002.
- [46] H.H. Horowitz, G. Metzger, *J. Anal. Chem.* 35 (1963) 1464–1468.
- [47] A.W. Coats, J.P. Redfern, *Nature* 20 (1964) 68–69.
- [48] G.O. Piloyan, T.D. Pyabonikar, C.S. Novikova, *Nature* 212 (1966) 1229–1304.
- [49] B.K. Singh, R.K. Sharma, B.S. Garg, *Spectrochim. Acta A* 63 (2006) 96–102.
- [50] R.G. Parr, P.K. Chattaraj, *J. Am. Chem. Soc.* 113 (1991) 1854–1855.
- [51] R.G. Parr, L.V. Szentpaly, S. Liu, *J. Am. Chem. Soc.* 121 (1999) 1922–1924.
- [52] P.K. Chattaraj, B. Maiti, U. Sarkar, *J. Phys. Chem. A* 107 (2003) 4973–4975.
- [53] R.G. Parr, R.A. Donnelly, M. Levy, W.E. Palke, *J. Chem. Phys.* 68 (1978) 3801–3807.
- [54] R.G. Parr, R.G. Pearson, *J. Am. Chem. Soc.* 105 (1983) 7512–7516.
- [55] R.G. Parr, W. Yang, *Density Functional Theory of Atoms and Molecules*, Oxford University Press, Oxford, UK, 1989.